Published in final edited form as:
J Control Release. 2006 July 20; 113(3): 226–235.

Delivery of Neurotrophin-3 from Fibrin Enhances Neuronal Fiber Sprouting After Spinal Cord Injury

Sara J. Taylor[a], **Ephron S. Rosenzweig**[b], **John W. McDonald III**[b,c,*], and **Shelly E. Sakiyama-Elbert**[a,d,e,#]

a*Department of Biomedical Engineering, Washington University, St. Louis, Missouri 63130, USA*

b*Restorative Treatment and Research Center, Department of Neurology, Washington University School of Medicine, St. Louis, MO, USA*

c*Department of Neurological Surgery and Anatomy and Neurobiology, Washington University School of Medicine, St. Louis, MO, USA*

d*Division of Plastic Surgery, Department of Surgery, Washington University School of Medicine, St. Louis, Missouri 63108, USA*

e*Center for Materials Innovation, Washington University, St. Louis, Missouri 63130, USA*

Abstract

Neurotrophins have been shown to promote axonal growth and regeneration after spinal cord injury. The therapeutic utility of neurotrophins may be enhanced by using a controlled delivery system to increase the duration of neurotrophin availability following injury. Such a delivery system can be incorporated into a bioactive scaffold to serve as a physical bridge for regeneration. This study assessed the effect of controlled delivery of neurotrophin-3 (NT-3) from fibrin scaffolds implanted in spinal cord lesions immediately following 2-mm ablation injury in adult rats. Nine days after injury, fibrin scaffolds containing the delivery system and NT-3 (1000 ng/mL) elicited more robust neuronal fiber growth into the lesion than did control scaffolds or saline (1.5- to 3-fold increase). Implantation of fibrin scaffolds resulted in a dramatic reduction of glial scar formation at the white matter border of the lesion. Hindlimb motor function of treated animals did not improve relative to controls at 12 weeks post-injury. Thus, controlled delivery of NT-3 from fibrin scaffolds enhanced the initial regenerative response by increasing neuronal fiber sprouting and cell migration into the lesion, while functional motor recovery was not observed in this model.

Keywords

controlled release; growth factor; nerve regeneration

Introduction

The ability of the adult spinal cord to regenerate after injury is limited; in order to restore functional connectivity, neurons must regenerate through a non-permissive environment that includes myelin-associated and glial scar-associated inhibitors and a cystic cavity. Neurotrophin 3 (NT-3) has been shown to promote neuronal regeneration when delivered to the site of spinal cord injury (SCI) by direct injection [1], osmotic mini-pumps [2], adenoviral

*Current affiliation: Kennedy Krieger Institute, Baltimore, Maryland and the Departments of Neurology, Neuroscience and Physical Medicine and Rehabilitation at Johns Hopkins School of Medicine, Baltimore, Maryland, 21205, USA
#To whom correspondence should be addressed: Department of Biomedical Engineering, Washington University Campus Box 1097, One Brookings Drive, St. Louis, MO 63130, USA Tel: +1 314 936 7556, Fax: +1 314 935 7448, e-mail: sakiyama@wustl.edu

vectors containing a neurotrophin gene [3], transgenic cells overexpressing a neurotrophin gene [4], and scaffolds soaked with neurotrophin [5,6]. This paper focuses on a strategy for delivering NT-3 in a controlled manner from fibrin scaffolds that can also serve as a physical bridge for regeneration.

When using protein drugs, such as neurotrophins, as therapeutic agents, several factors, such as loss into the cerebrospinal fluid, proteolysis, or aggregation, may reduce the efficacy of the drug. The use of a delivery system that sequesters and protects the protein until the appropriate time of release can allow the drug to be available to regenerating cells over a longer period of time, which is particularly important in the case of nerve regeneration (which occurs over several weeks). In contrast to polymer-based delivery systems [7,8], which use physical entrapment of the neurotrophin to provide sustained release in the central nervous system [9-11], in this work, an affinity-based delivery system is used to provide sustained release of NT-3 from fibrin scaffolds [12,13].

In this delivery system (Figure 1), a synthetic bi-domain peptide is covalently crosslinked to fibrin during polymerization [14] and can also bind to heparin via electrostatic interactions [15], thereby immobilizing heparin within the fibrin scaffold. Heparin can, in turn, bind to growth factors that contain heparin-binding domains or growth factors, such as nerve growth factor (NGF) or NT-3, with basic domains [12]. By this series of non-covalent interactions, growth factors can be immobilized within fibrin scaffolds, thereby limiting the release of growth factors by diffusion [12,13,16]. Following plasmin-mediated degradation of the scaffold by infiltrating cells, like neurons [17,18], fibrin-bound growth factor is released and made available for action on nearby cells.

The delivery of growth factors from the HBDS has been shown to enhance neurite outgrowth *in vitro* [12,13,16] and neuronal fiber sprouting *in vivo* [16,19] A preliminary *in vivo* SCI study qualitatively showed increased neuronal fiber infiltration of the lesion when treated with fibrin containing the HBDS and NT-3 compared to those with unmodified fibrin at 9 days post-implantation [16]. A more rigorous study is necessary to examine the effect of dose of NT-3 on neuronal fiber sprouting in a quantitative manner, the effect of the delivery system on glial scar formation, and the potential of this treatment to promote functional motor recovery. Here, the neuroanatomical effects of fibrin scaffolds containing various doses of NT-3 with the delivery system were evaluated 9 days after SCI. Locomotor function was assessed for 12 weeks to investigate the ability of controlled delivery of NT-3 to enhance functional recovery in this model of SCI.

Materials and Methods

Preparation of Fibrin Scaffolds

All materials were purchased from Fisher Scientific (Pittsburgh, PA) unless otherwise noted. Fibrin scaffolds were made as described previously [13] by mixing the following components: human plasminogen-free fibrinogen (4 mg/mL, Sigma, St. Louis, MO), $CaCl_2$ (2.5 mM), and thrombin (2 NIH units/mL, Sigma) in Tris-buffered saline (TBS, 137 mM NaCl, 2.7 mM KCl, 33 mM Tris, pH 7.4). The bi-domain peptide, denoted $\alpha_2PI_{1\text{-}7}$-$ATIII_{121\text{-}134}$, was synthesized by standard solid phase Fmoc chemistry as described previously [20] with the amino acid sequence dL**NQEQVSPK**(βA)FAKLAARLYRKA-NH_2, where dL denotes dansyl leucine, bold residues indicate the Factor XIIIa substrate [14], and the italicized residues indicate the heparin-binding sequence [15]. In scaffolds containing the delivery system, $\alpha_2PI_{1\text{-}7}$-$ATIII_{121\text{-}134}$ peptide (0.23 mM) and heparin (6 μM, Sigma, sodium salt from porcine intestinal mucosa) were added to the fibrin polymerization mixture (total volume of 200 μl). Recombinant human NT-3 (at various concentrations, see below, Peprotech, Rocky Hill, NJ) was added in some groups to the polymerization mixture. Small beads of fibrin (1 mm diameter)

were formed by ejecting the polymerization mixture from a 29-gauge needle onto a sterile surface. The beads were allowed to polymerize at room temperature for 30 min before implantation.

In vivo Studies-Rat Suction Ablation SCI Model

All experimental procedures on animals complied with the Guide for the Care and Use of Laboratory Animals and were performed under the supervision of the Division of Comparative Medicine at Washington University. Ablation of a 2-mm section of the spinal cord at T9 was performed using suction as described previously [16]. Briefly adult, female Long Evan rats (250-275 g, Charles River, Wilmington, MA) were anesthetized, and a dorsal laminectomy at T9 was performed to expose the spinal cord. A 2 mm section of the spinal cord was aspirated using a suction tube (Baron, 3 French, Biomedical Research Instruments, Rockville, MD) attached to a vacuum pump, leaving a complete gap between the rostral and caudal spinal cord segments. A sterile fibrin scaffold with or without the delivery system and/or NT-3 was placed in the gap. In the 9-day study, experimental groups received fibrin with the delivery system and NT-3 (NT-3 concentrations of 50, 100, 250, 500, and 1000 ng/mL, group referred to as F-DS-NT3(x) where x indicates the concentration of NT-3 in ng/mL). Control groups received either fibrin (without the delivery system) with NT-3 concentrations of 100 or 1000 ng/mL (referred to as F-NT3(x), where x indicates the concentration of NT-3 in ng/mL), fibrin containing the delivery system and no NT-3 (referred to as F-DS), unmodified fibrin (referred to as F-only), or sterile TBS (total of 10 groups, 6-8 animals per group). In the 12-week study, the three treatment groups received sterile TBS injection, fibrin containing NT-3 (1000 ng/mL), and fibrin containing the delivery system and NT-3 (1000 ng/mL) (total of 3 groups, 8-10 animals per group).

Animals were given cefazolin (15 mg/kg, twice a day) for the duration of the 9-day study and for the first 14 days of the 12-week study as a prophylactic against urinary tract infections. Bladders were expressed manually twice a day; animals did not regain bladder function within 12 weeks.

The animals were euthanized 9 days or 12 weeks post-operatively. After transcardial perfused using 4% paraformaldehyde, spinal cords were dissected and processed as described previously [16]. Briefly, frozen samples were cut into 20 μm longitudinal sections and processed for immunohistochemistry.

Basso-Beattie-Bresnahan (BBB) Open Field Locomotor Testing

Hindlimb function was assessed weekly after injury using the BBB locomotor rating scale in an open field (2 x 4 feet) [21]. Rats were observed for 4 min by a trained observer, and each hindlimb was scored individually from 0 (no observable movements) to 21 (normal gait).

Immunohistochemistry

Immunohistochemistry was performed as described previously [16]. Briefly, sections permeabilized with 0.1% Triton-X 100 and blocked with for with 10% BSA (bovine serum albumin) and 3% normal goat serum (NGS, Sigma). The following primary antibodies were used: glial fibrilliary acidic protein (GFAP, rabbit polyclonal, recognizing astrocytes, 1:4, ImmunoStar, Hudson, WI), neuronal class III β-tubulin (Tuj1, mouse monoclonal, recognizing neurons, 1:500, Covance Research Products, Inc., Berkeley, CA), ED-1 (mouse monoclonal, recognizing macrophages, 1:100, Serotec, Oxford, UK), calcitonin gene related peptide (CGRP, rabbit polyclonal, recognizing sensory neurons, 1:4000, Chemicon, Temecula, CA), serotonin (5-HT, rabbit polyclonal, recognizing raphespinal tract neurons, 1:15,000, Immunostar), neuronal nuclei (NeuN, mouse monoclonal, 1:500, Chemicon). Goat anti-rabbit or goat anti-mouse secondary antibodies (Alexa Fluor 488 conjugated, 1:300, Molecular

Probes) were used. For staining using choline acetyltransferase (ChAT, goat polyclonal, recognizing primary cholinergic motor neurons, 1:50, Chemicon), rabbit serum (Sigma) was used instead of NGS. All sections were stained with Hoechst 33258 (1:1000, Molecular Probes) and mounted with ProLong Antifade reagent (Molecular Probes).

For double staining, sections were stained first with rabbit polyclonal GFAP antibody, then with mouse monoclonal Tuj1 antibody. Secondary antibodies (goat anti-rabbit Alexa Fluor 488 and goat anti-mouse Alexa Fluor 555) were highly cross adsorbed against other species (Molecular Probes).

Quantification of Neuronal Fiber Density, Astroglial Scar Formation, and Macrophage/ Microglia Density

For quantification of neuronal fibers, which were stained with the β-tubulin III (Tuj1) antibody, the lesion area was imaged at 40 x magnification using an Olympus IX70 microscope (Olympus America, Melville, NY) and Magnafire camera (Optronics, Goleta, CA). Individual smaller images were spliced together using Photoshop (Adobe, San Jose, California) to yield a complete picture of the lesion area and surrounding intact cord. The density of Tuj1 stained sections was quantified inside the lesion area using Ia32 software (Leco, St. Joseph, MI). The border of the lesion was defined by referencing the GFAP-positive area (indicating the astroglial scar) in adjacent sections. An intensity threshold was set so that only Tuj1-positive neuronal fibers were quantified. Because encroaching dorsal roots did not represent neuronal fiber sprouting from the spinal cord stumps, Tuj1 staining of these structures was not included in the analysis of any treatment group. Tuj1 density was quantified separately in three equal sections: the rostral, middle and caudal thirds of the lesion. The area of positive Tuj1 staining (the number of pixels in which the intensity was above the set intensity threshold) was divided by the total number of pixels in each of the three investigated regions to yield Tuj1 density. All statistics were performed with Analysis of Variance (ANOVA, planned comparison post-hoc test) using Statistica (StatSoft, Tulsa, OK).

The density of GFAP labeling of the astroglial was quantified separately inside the white and gray matter that bordered the lesion in the TBS, F-only, F-DS, F-NT3(1000 ng/mL), and F-DS-NT3(1000 ng/mL) groups. Images were analyzed using Ia32 software (200 x magnification, four per animal at white matter border, two per animal at gray matter border). An intensity threshold was set so that only areas positive for GFAP were quantified. The area of GFAP staining (the number of pixels in which the intensity was above the set intensity threshold) was divided by the total number of pixels in the area of the picture to yield GFAP density.

ED-1 staining of macrophages and microglia was analyzed inside the lesion and in adjacent white matter in the TBS, F-only, F-DS, F-NT3(1000 ng/mL), and F-DS-NT3(1000 ng/mL) groups using Image-Pro Express software (MediaCybernetics, Silver Spring, MD). In TBS-treated cords, density was assessed in tissue adjacent to the central cavity; in fibrin scaffold-treated cords, density was assessed in tissue adjacent to but not including the fibrin remnants. All ED-1-positive cells containing a nucleus were counted in a 200 x magnification picture; the count was divided by the area of the picture to yield macrophage/microglia density.

Results

9-day Neuroanatomical Study

The ability of fibrin scaffolds containing the HBDS and NT-3 to influence regeneration was evaluated at 9 days after SCI. Studies performed previously in collaboration with Martin Schwab (University of Zurich) where fibrin scaffolds were implanted after spinal cord dorsal hemisection showed that fibrin was present at 10 days but degraded by 14 days (Sakiyama and

Schwab, unpublished results). Therefore, a 9-day time point was chosen in order to study the acute effects of the fibrin scaffold while it is still present in the injury environment. Previously, 100 ng/mL of NT-3 was found to be the optimal dose for promoting neurite outgrowth *in vitro* [16]; therefore, we investigated doses surrounding this optimal *in vitro* dose.

Neuronal Fiber Sprouting

Tuj1 staining was performed to assess the effect of fibrin scaffolds on neuronal fiber sprouting. GFAP staining was used as an indicator of the lesion border; the lesion size in all cords was observed to be 2-3 mm in length at 9 d. Neuronal fiber sprouting into the lesion area was dramatically different between experimental groups. In the TBS group, very few neuronal fibers sprouted into the lesion area; most fibers ended abruptly at the lesion border (Figure 2A). In contrast, fibrin-treated groups showed neuronal fiber infiltration of the lesion site, both at the border of the intact cord and well inside the lesion (Figure 2B, C, D). Fibrin remnants frequently remained inside the lesion area (as visualized by dansyl-labeled peptide in the HBDS), and neuronal fibers were observed touching the borders of fibrin remnants (not shown). In the F-DS-NT3(1000 ng/mL) group, particularly dense neuronal fiber staining was observed (inset, Figure 2D). Although neuronal fibers infiltrated the lesion, neuron cell bodies (NeuN, neuronal nuclear, staining) were not observed in the lesion (all treatment groups, data not shown).

Differences in neuronal fiber density between treatment groups were quantified in the whole lesion and in three equal-area regions of lesion separately (rostral, middle, and caudal thirds) (Figure 2E). For reference, the Tuj1 density of normal cords was measured to be ~5% in white matter, ~80% in gray matter, and 40% overall. The overall (whole lesion) neuronal fiber density in the TBS-treated lesions was 3%. For control groups containing fibrin scaffolds, overall neuronal fiber density in the lesion was ~6-7%. In the F-DS-NT3(1000 ng/mL) treatment group, the overall neuronal fiber density in the lesion was 10.4%, which represents a ~1.5-fold increase over control groups containing fibrin, and a 3-fold increase over the TBS-treated group. Overall neuronal fiber density in the F-DS-NT3(1000 ng/mL) was higher than overall neuronal fiber density in the F-NT3(1000 ng/mL) group, where no delivery system was present (7%, 1.5-fold increase). This trend was most pronounced in the rostral third of the lesion; in both the F-DS-NT3(500 ng/mL) (14%) and F-DS-NT3(1000 ng/mL) (15%) groups, rostral fiber density was greater than in the F-NT3(1000 ng/mL) group (7%), representing a 2-fold increase. These results indicate that NT-3 delivery from the HBDS enhanced neuronal fiber density relative to NT-3 delivery from unmodified fibrin scaffolds, especially at the rostral edge of the lesion, where spouting of supraspinal axons would be anticipated.

Glial Scar Formation

To assess the formation of the glial scar, astrocyte staining (using an antibody to GFAP) was performed. In the TBS group, astrocyte density was high at both the gray matter (which contains neuronal and glial cell bodies) and white matter (which contains axonal tracts) border of the lesion (Figure 3A). This indicates the formation of a dense astroglial scar surrounding the lesion, which poses as significant biochemical barrier to regenerating axons. However, in fibrin scaffold-treated groups, astrocyte density appeared to be reduced, particularly at the border of the white matter with the lesion (arrowheads in Figure 3A and D). Reduced scar formation, particularly at the white matter border, is important for the regeneration of long axonal tracts, such as those of the corticospinal tract. To investigate this difference, GFAP density was quantified at the white matter and the gray matter lesion borders in five treatment groups, TBS, F-only, F-DS, F-NT3(1000 ng/mL), and F-DS-NT3(1000 ng/mL). Figure 3E shows that astrocyte density at the white matter border was significantly lower in fibrin scaffold-treated groups than in the TBS group. Astrocyte density at the gray matter border with the lesion did

not show a difference between the TBS and fibrin scaffold-treated groups. Thus, implantation of fibrin scaffolds appears to decrease scar formation at the white matter border of the lesion.

Migration into the Lesion

In order to investigate the relationship between neuronal fibers and astrocytes, we performed double staining with Tuj1 and GFAP antibodies. In TBS-treated cords, dense astrocyte staining at the border of the lesion was associated failure of Tuj1-positive neuronal fibers to extend into the lesion. In contrast, in the F-DS-NT3(1000 ng/mL) treated cords, neuronal fibers and long astrocyte processes (arrowhead) occurred along channel-like formations connecting the lesion to the intact cord (Figure 4B). Astrocytes were not frequently present within the lesion. Other fibrin scaffold-treated groups showed similar results (data not shown), suggesting that fibrin scaffolds may reduce scar density and encourage longitudinal regeneration of neuronal fibers and astrocytes along channel-like formations connecting the lesion with the intact cord.

Macrophage/Microglia Infiltration

The effect of fibrin scaffold treatment on macrophage/microglia infiltration was assessed as an indication of inflammation. Macrophages and microglia were present surrounding the lesion in all treatment groups (Figure 5A, B). In cords treated with fibrin scaffolds, ED-1-positive cells were present just inside the lesion in areas between neuronal fiber channel-like formations connecting the lesion to the intact cord. ED-1 staining was particularly dense at the white matter border of the lesion (Figure 5B, arrowhead and Figure 5C), where the cells appeared vacuolated and phagocytic. Macrophages/microglia were also present around remnants of fibrin (F), where they were smaller and did not appear vacuolated (Figure 5D). The macrophage/microglia density inside the lesion and surrounding the lesion was compared between treatment groups (Figure 5E). No difference in macrophage/microglia density was observed between treatment groups, indicating that the presence of fibrin does not increase the density of macrophage/microglia inside or surrounding the lesion. In all treatment groups, the density in the white matter bordering the intact cord was greater than inside the lesion, indicating that macrophages/microglia are more attracted to surrounding white matter than to the lesion itself. Therefore, the presence of fibrin scaffolds did not increase the density of macrophage/microglia inside the lesion or in the intact cord bordering the lesion.

Sprouting of Neuronal Subpopulations

To determine the effects of fibrin scaffold treatment on different neuronal subpopulations, the regenerative responses of ascending sensory neurons (CGRP), primary spinal motoneurons (ChAT), and neurons of the raphespinal tract (5-HT) were investigated. The CGRP-positive sensory fibers were found in encroaching dorsal roots, the intact dorsal spinal cord, and inside the lesion. In the TBS-treated cords, CGRP-positive fibers were present at the border of the gray matter (GM) with the lesion (Figure 6A), but were rarely observed sprouting past the astroglial scar at the lesion border. In all fibrin scaffold-treated groups, CGRP-positive fibers were observed sprouting beyond the border with the lesion (Figure 6B). However, the density of CGRP-positive fibers was much lower than the density of Tuj1-positive fibers; therefore, sensory neuron fibers do not make up the majority of the neuronal fibers present in the lesion site and at the lesion borders.

The ChAT antibody stains large neuronal cell bodies located within ventral gray matter (spinal cord alpha motoneurons). Fewer ChAT-positive fibers sprouted into the lesion in the TBS group (Figure 6C) than in the fibrin scaffold-treated groups (Figure 6D, F-DS-NT3 (1000ng/mL) shown). In all fibrin scaffold-treated groups, ChAT fiber staining was evident inside the lesion at the rostral and caudal edges of the lesion and in the middle of the lesion near fibrin remnants (data not shown). The density of ChAT-positive fibers was observed to be comparable

to the density of Tuj1-positive fibers, indicating that ChAT-positive fibers were a major contributor to the population of Tuj1-positive fibers in fibrin-scaffold treated cords.

The regenerative response of serotonergic neurons was investigated using 5-HT staining. Sprouting of serotonergic neurons into the lesion was not observed in the lesion of the TBS-treated cords (Figure 6E), whereas sprouting into the lesion was seen in all fibrin scaffold-treated groups (Fig. 6F). Notably, this sprouting did not continue more than 500 μm into the lesion. The density of 5-HT-positive fibers was much lower than the density of Tuj1-positive fibers; therefore, serotonergic fibers did not make up the majority of the neuronal fibers present at the lesion site.

In summary, fibrin scaffolds significantly enhanced the regenerative environment by decreasing the astroglial scar formation at the white matter border of the lesion. Furthermore, the controlled release of NT-3 with the HBDS resulted in greater neuronal fiber sprouting than other fibrin scaffold treatments after 9 days.

Functional Regeneration Study (12 weeks)

The effect of the controlled release of NT-3 on functional regeneration was assessed for 12 weeks. Immediately after injury, one of three treatments was administered: TBS, F-NT3(1000 ng/mL), or F-DS-NT3(1000 ng/mL). Because of the requirement for prolonged animal care and the need for larger group sizes, a complete set of control treatments (including F-only, F-DS groups) was not performed.

In order to assess the effect of treatment on functional ability, BBB open field motor testing [21] was performed weekly (Figure 7). Immediately after injury, animals had no hindlimb function (score of 0). One week after injury, animals had regained slight or extensive movement of two or three hindlimb joints (BBB score of 2-3). At 12 weeks, most animals had regained sweeping motion or plantar paw placement of their hindlimbs (BBB score of 8). Some animals had regained plantar placement of their hindpaw with weight support or occasional weight supported plantar steps (score of 9-10). However, no differences in functional motor recovery were observed between the treatment groups.

Upon histological examination, the lesion in all groups was much larger at 12 weeks than at 9 days (5 mm vs. 2-3 mm in length), largely due to formation of cystic cavities at the rostral and caudal borders of the lesion (data not shown).

Discussion

The most significant finding of this study was that the controlled delivery of NT-3 from fibrin scaffolds using the HBDS enhanced neuronal fiber sprouting compared to the delivery of NT-3 from unmodified fibrin scaffolds 9 days after injury. NT-3 is known to be a powerful neurotropic agent, and point sources and concentration gradients of NT-3 can induce turning response from growth cones of various types of neurons [22,23]. Release of NT-3, which can occur in this system by diffusion of unbound NT-3 or by release of bound NT-3 by degradation of the scaffold, can direct neuronal growth toward and into the lesion. The amount of NT-3 released by dissociation and diffusion from the fibrin scaffold can be tuned by varying the heparin concentration and is approximately 60% of the total NT-3 with the heparin concentrations used in this study [16]. This type of release could stimulate the recruitment of cells from outside the scaffold and induce neuronal fiber extension into the lesion area. The remaining NT-4 (40%) can be release by cell-mediate degradation of the fibrin scaffold. In the current study, fibrin remnants were still present nine days after implantation. Therefore, fibrin scaffolds containing the delivery system continues to be a source for NT-3 release for at least 9 days.

All fibrin scaffolds enhanced the sprouting of peptidergic sensory fibers (CGRP), cholinergic alpha motor neurons (ChAT), and serotonergic neurons of the raphespinal tract (5-HT). NT-3 treatment did not qualitatively enhance the spouting of these neuronal subpopulations. Only alpha motor neurons were seen inside the lesion cavity in fibrin-scaffold treated groups in significant numbers. This result is of benefit for trying to stimulate regeneration of motor fibers while limiting the regeneration of nociceptive, pain-responsive sensory fibers (stained with CGRP) that may cause exacerbated pain sensations. In previous studies using NT-3 in combination with BDNF or fetal spinal cord tissue transplants, regeneration of injured raphespinal neurons is enhanced when assessed at greater time delays than 9-days; these studies also use NT-3 at much greater amounts than used here [24,25]. Other subpopulations of neurons are known to be responsive to NT-3, such as neurons of the corticospinal tract and the ascending dorsal columns [1,26]; these populations can not be examined by immunohistochemical techniques and should be examined in future long term studies.

In this study, implantation of fibrin scaffolds decreased astrocyte density at the border of the lesion with intact white matter and affected the morphology of astrocytes near the lesion border. It should be noted that because GFAP staining was used as an indicator of the boundaries of the lesion, the relative absence of GFAP staining in fibrin scaffold-treated groups could influence the perceived lesion size. However, lesion size did not vary between treatment groups (data not shown). In fibrin scaffold-treated groups, elongated astrocyte processes crossing the lesion border formed an environment more likely to permit sprouting, in contrast to densely clustered astrocytes at the lesion border in the TBS-treated group. Neuronal fibers extended in close proximity to these elongated astrocyte processes in channel-like formations that connected the intact cord with the lesion, as well as inside the lesion. Similar results have been noted in another study [27], in which astrocytes were present in channel-like formations associated with growth of neuronal fibers into lesion areas.

While the regenerative attempt in the short-term *in vivo* study was increased, functional recovery was not observed in animals treated with fibrin scaffolds containing NT-3 with or without the delivery system after injury. The lesion size also expanded significantly from 9d to 12 weeks, with large cystic cavities located at the rostral and caudal areas of the lesion. At 9 days, the areas immediately rostral and caudal to the lesion were dense with macrophages/microglia, indicating that the inflammatory process was ongoing. Similar cavity formation in the rostral and caudal areas of a lesion was seen in a study where fibrin glue served as a control treatment in a complete 4-mm transection model; tissue sparing of the cord adjacent to fibrin implants decreased from around 75% at 2 weeks to about 40% at 8 weeks [28]. In future studies, lesion expansion caused by inflammation might be decreased with agents such as methylprednisolone [29].

While acutely implanted fibrin scaffolds increased neuronal fiber sprouting, decreased glial scar formation after 9 days, this treatment alone was not sufficient to reduce the secondary injury damage observed at 12 weeks in this severe injury model. Previous studies indicate that fibrin is degraded within 14 days after implantation (Schwab and Sakiyama, unpublished results). It is possible that the time-course of fibrin degradation does not prolong the availability of NT-3 long enough to counteract the continuing degeneration observed in this injury model. Increasing fibrin density or incorporating inhibitors of plasmin degradation into the scaffold might increase the time fibrin is present in the cord; however, the effect of these changes on the ability of cells and neuronal fibers to infiltrate the scaffold and release NT-3 would have to be carefully studied, as these actions are plasmin-dependent as well. Further investigation of regenerative potential of controlled delivery of NT-3 from fibrin scaffolds alone in or combination with other therapies, such as embryonic stem cell implantation, should be examined in the future using a less severe injury model, such as a dorsal hemisection or contusion, and/or treatment in the chronic phase after the lesion has stabilized.

Acknowledgements

Thanks to Amanda McKee for surgical assistance, Dr. Daniel Becker and Dr. Michael Howard for instruction on the SCI model, Dr. Lawrence Schramm, Dr. Frank Schottler, and Urvi Lee for helpful discussions, Daniel Hunter for analysis assistance, and Suellen Greco and Isabel Acevado for help with veterinary care. The authors acknowledge the Whitaker Foundation for graduate fellowship support (SJT) and the NIH-NINDS for funding (R01 NS51454).

References

1. Schnell L, Schneider R, Kolbeck R, Barde YA, Schwab ME. Neurotrophin-3 enhances sprouting of corticospinal tract during development and after adult spinal cord lesion. Nature 1994;367(6459):170–3. [PubMed: 8114912]
2. Bradbury EJ, Khemani S, Von, King R, Priestley JV, McMahon SB. NT-3 promotes growth of lesioned adult rat sensory axons ascending in the dorsal columns of the spinal cord. Eur J Neurosci 1999;11 (11):3873–83. [PubMed: 10583476]
3. Zhou L, Baumgartner BJ, Hill-Felberg SJ, McGowen LR, Shine HD. Neurotrophin-3 expressed in situ induces axonal plasticity in the adult injured spinal cord. J Neurosci 2003;23(4):1424–31. [PubMed: 12598631]
4. Grill R, Murai K, Blesch A, Gage FH, Tuszynski MH. Cellular delivery of neurotrophin-3 promotes corticospinal axonal growth and partial functional recovery after spinal cord injury. J Neurosci 1997;17 (14):5560–72. [PubMed: 9204937]
5. Houweling DA, Lankhorst AJ, Gispen WH, Bar PR, Joosten EA. Collagen containing neurotrophin-3 (NT-3) attracts regrowing injured corticospinal axons in the adult rat spinal cord and promotes partial functional recovery. Exp Neurol 1998b;153(1):49–59. [PubMed: 9743566]
6. Iwaya K, Mizoi K, Tessler A, Itoh Y. Neurotrophic agents in fibrin glue mediate adult dorsal root regeneration into spinal cord. Neurosurgery 1999;44(3):589–95. [PubMed: 10069596]discussion 595-6
7. Goraltchouk A, Scanga V, Morshead CM, Shoichet MS. Incorporation of protein-eluting microspheres into biodegradable nerve guidance channels for controlled release. J Control Release 2006;110(2): 400–7. [PubMed: 16325953]
8. Yang Y, De Laporte L, Rives CB, Jang JH, Lin WC, Shull KR, Shea LD. Neurotrophin releasing single and multiple lumen nerve conduits. J Control Release 2005;104(3):433–46. [PubMed: 15911044]
9. Powell EM, Sobarzo MR, Saltzman WM. Controlled release of nerve growth factor from a polymeric implant. Brain Res 1990;515(12):309–11. [PubMed: 2357568]
10. Hoffman D, Wahlberg L, Aebischer P. NGF released from a polymer matrix prevents loss of ChAT expression in basal forebrain neurons following a fimbria-fornix lesion. Exp Neurol 1990;110(1): 39–44. [PubMed: 2209780]
11. Saltzman WM, Mak MW, Mahoney MJ, Duenas ET, Cleland JL. Intracranial delivery of recombinant nerve growth factor: release kinetics and protein distribution for three delivery systems. Pharm Res 1999;16(2):232–40. [PubMed: 10100308]
12. Sakiyama-Elbert SE, Hubbell JA. Controlled release of nerve growth factor from a heparin-containing fibrin-based cell ingrowth matrix. J Control Release 2000a;69(1):149–58. [PubMed: 11018553]
13. Sakiyama-Elbert SE, Hubbell JA. Development of fibrin derivatives for controlled release of heparin-binding growth factors. J Control Release 2000b;65(3):389–402. [PubMed: 10699297]
14. Ichinose A, Tamaki T, Aoki N. Factor XIII-mediated cross-linking of NH2-terminal peptide of alpha 2-plasmin inhibitor to fibrin. FEBS Lett 1983;153(2):369–71. [PubMed: 6617867]
15. Tyler-Cross R, Sobel M, Marques D, Harris RB. Heparin binding domain peptides of antithrombin III: analysis by isothermal titration calorimetry and circular dichroism spectroscopy. Protein Sci 1994;3(4):620–7. [PubMed: 8003980]
16. Taylor SJ, McDonald JW 3rd, Sakiyama-Elbert SE. Controlled release of neurotrophin-3 from fibrin gels for spinal cord injury. J Control Release 2004;98(2):281–94. [PubMed: 15262419]
17. Herbert CB, Bittner GD, Hubbell JA. Effects of fibinolysis on neurite growth from dorsal root ganglia cultured in two- and three-dimensional fibrin gels. J Comp Neurol 1996;365(3):380–91. [PubMed: 8822177]

18. Pittman RN, Ivins JK, Buettner HM. Neuronal plasminogen activators: cell surface binding sites and involvement in neurite outgrowth. J Neurosci 1989;9(12):4269–86. [PubMed: 2512375]

19. Lee AC, Yu VM, Lowe JB 3rd, Brenner MJ, Hunter DA, Mackinnon SE, Sakiyama-Elbert SE. Controlled release of nerve growth factor enhances sciatic nerve regeneration. Exp Neurol 2003;184 (1):295–303. [PubMed: 14637100]

20. Sakiyama SE, Schense JC, Hubbell JA. Incorporation of heparin-binding peptides into fibrin gels enhances neurite extension: an example of designer matrices in tissue engineering. Faseb J 1999;13 (15):2214–24. [PubMed: 10593869]

21. Basso DM, Beattie MS, Bresnahan JC. A sensitive and reliable locomotor rating scale for open field testing in rats. J Neurotrauma 1995;12(1):1–21. [PubMed: 7783230]

22. Paves H, Saarma M. Neurotrophins as in vitro growth cone guidance molecules for embryonic sensory neurons. Cell Tissue Res 1997;290(2):285–97. [PubMed: 9321690]

23. Cao X, Shoichet MS. Investigating the synergistic effect of combined neurotrophic factor concentration gradients to guide axonal growth. Neuroscience 2003;122(2):381–9. [PubMed: 14614904]

24. Tobias CA, Shumsky JS, Shibata M, Tuszynski MH, Fischer I, Tessler A, Murray M. Delayed grafting of BDNF and NT-3 producing fibroblasts into the injured spinal cord stimulates sprouting, partially rescues axotomized red nucleus neurons from loss and atrophy, and provides limited regeneration. Exp Neurol 2003;184(1):97–113. [PubMed: 14637084]

25. Bregman BS, McAtee M, Dai HN, Kuhn PL. Neurotrophic factors increase axonal growth after spinal cord injury and transplantation in the adult rat. Exp Neurol 1997;148(2):475–94. [PubMed: 9417827]

26. Zhang Y, Dijkhuizen PA, Anderson PN, Lieberman AR, Verhaagen J. NT-3 delivered by an adenoviral vector induces injured dorsal root axons to regenerate into the spinal cord of adult rats. J Neurosci Res 1998;54(4):554–62. [PubMed: 9822165]

27. Ramer LM, Au E, Richter MW, Liu J, Tetzlaff W, Roskams AJ. Peripheral olfactory ensheathing cells reduce scar and cavity formation and promote regeneration after spinal cord injury. J Comp Neurol 2004;473(1):1–15. [PubMed: 15067714]

28. Patist CM, Mulder MB, Gautier SE, Maquet V, Jerome R, Oudega M. Freeze-dried poly(D,L-lactic acid) macroporous guidance scaffolds impregnated with brain-derived neurotrophic factor in the transected adult rat thoracic spinal cord. Biomaterials 2004;25(9):1569–82. [PubMed: 14697859]

29. Bracken MB, Shepard MJ, Collins WF, Holford TR, Young W, Baskin DS, Eisenberg HM, Flamm E, Leo-Summers L, Maroon J, et al. A randomized, controlled trial of methylprednisolone or naloxone in the treatment of acute spinal-cord injury. Results of the Second National Acute Spinal Cord Injury Study. N Engl J Med 1990;322(20):1405–11. [PubMed: 2278545]

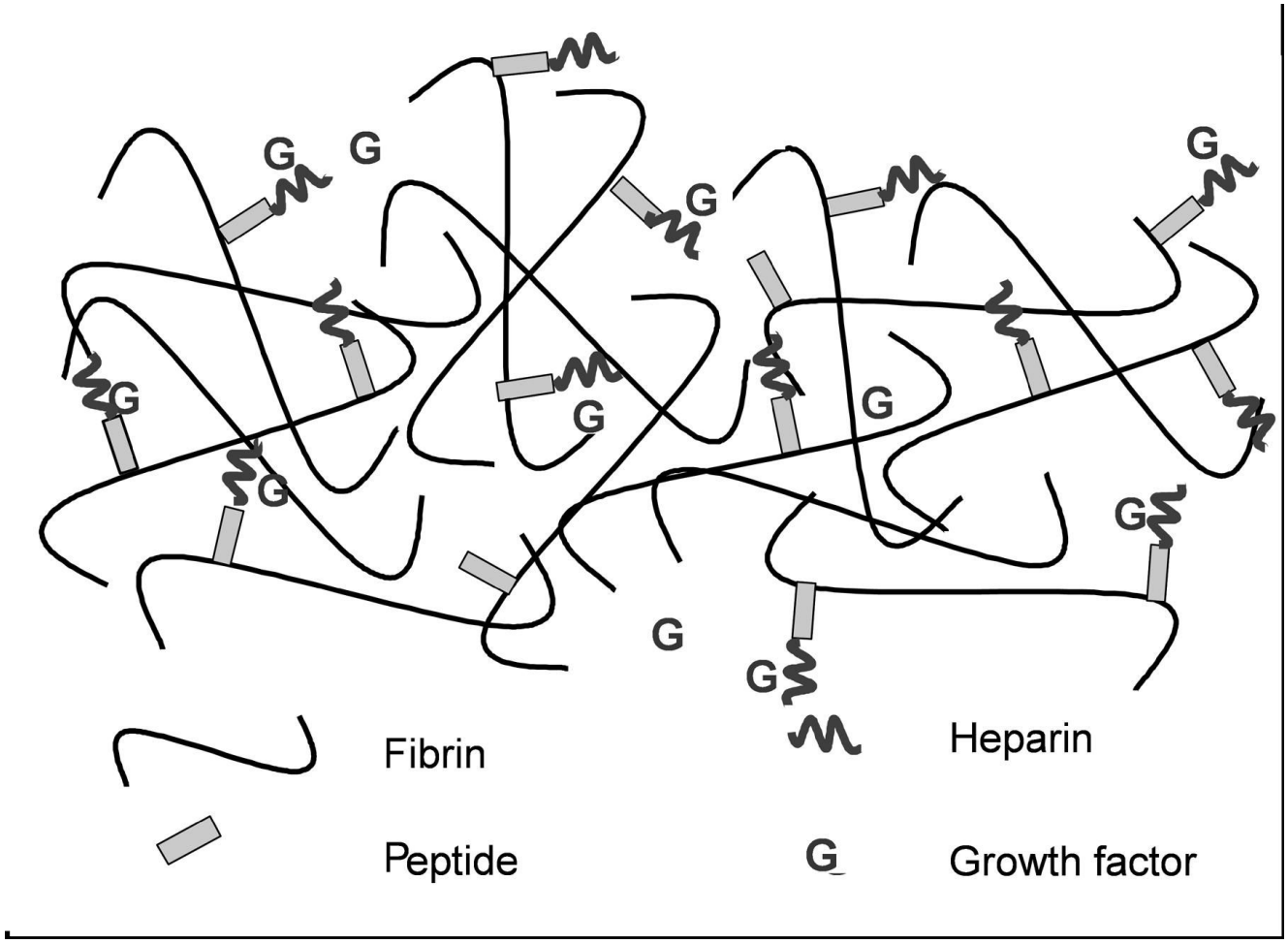

Figure 1.

A schematic diagram of the heparin binding delivery system (HBDS). The $\alpha_2PI_{1\text{-}7}$-$ATIII_{121\text{-}134}$ peptide is covalently crosslinked to the fibrin scaffold by Factor XIIIa. The peptide also binds heparin via electrostatic interactions. Heparin can bind growth factors such as bFGF, NGF, or NT-3, thereby sequestering the growth factors into the fibrin scaffold and limiting their loss from the scaffold by diffusion.

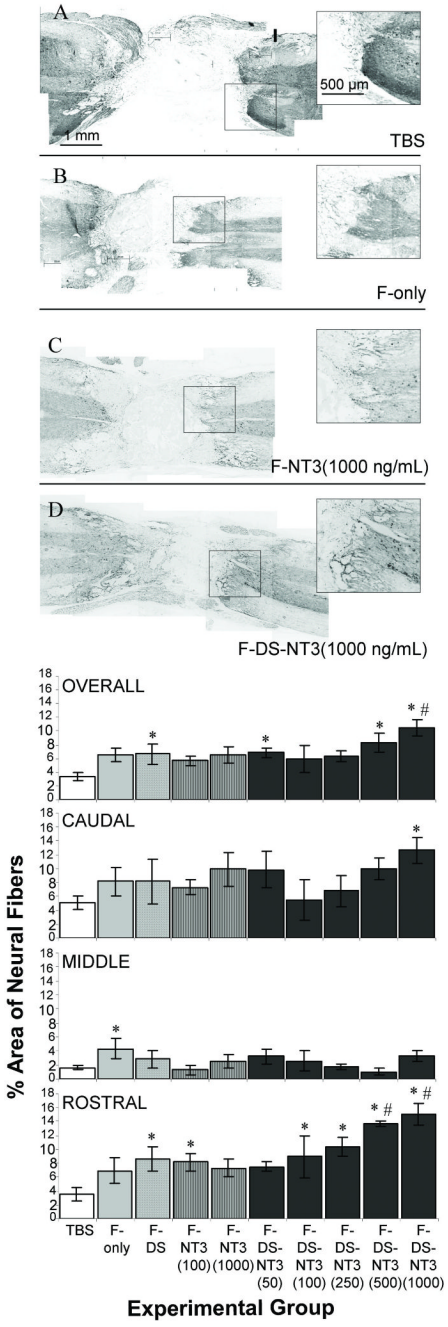

Figure 2.

Effect of controlled delivery of NT-3 from fibrin scaffolds on neuronal fiber sprouting. **A-D**. Neuronal staining (Tuj1) in spinal cords after treatment with (**A**) TBS, (**B**) fibrin (F-only), (**C**) fibrin and NT-3 at 1000 ng/mL (F-NT3(1000 ng/mL)), and (**D**) fibrin with the delivery system and NT-3 at 1000 ng/mL (F-DS-NT3(1000 ng/mL)). Horizontal sections, with the rostral cord oriented toward the right. Box indicates area of inset. F-DS-NT-3(1000 ng/mL) treated cords (**D**) show extensive neural sprouting (inset). **E**. Density of neuronal fiber sprouting in lesion areas of injured spinal cords in the whole lesion (overall) and in the caudal, middle, and rostral thirds of the lesion. * denotes $p<0.05$ vs. TBS group. # indicates $p<0.05$ vs. F-NT-3(1000 ng/mL) group. Error bars represent standard error of the mean.

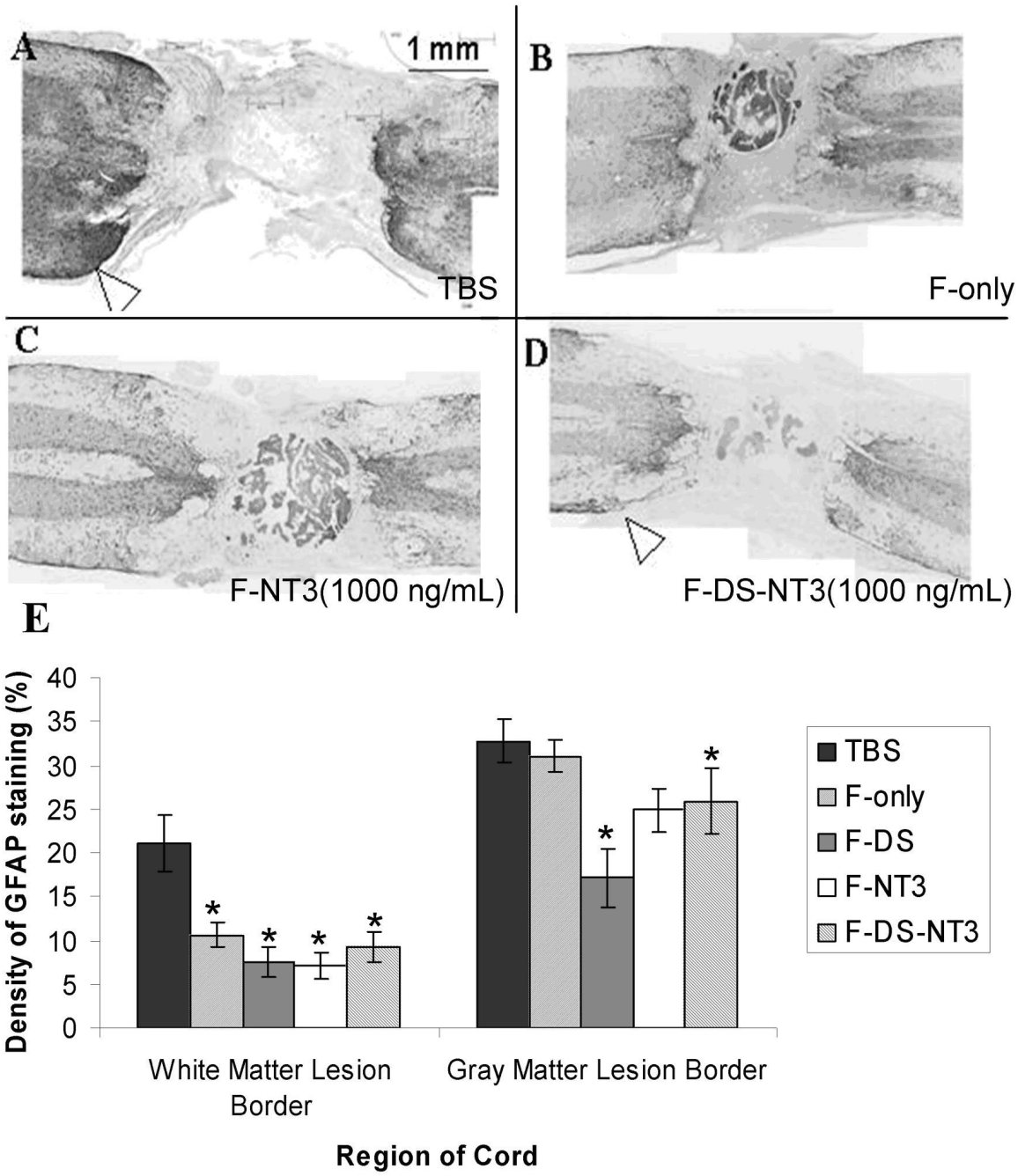

Figure 3.

Effect of fibrin scaffolds on astrocytes at the lesion border. **A-D**. Astrocyte staining (GFAP) of spinal cords after treatment with (**A**) TBS, (**B**) fibrin (F-only), (**C**) F-NT3(1000 ng/mL), and (**D**) F-DS-NT3(1000 ng/mL). Horizontal sections, with the rostral cord oriented toward the right. Arrowhead indicates dense astrocyte network around lesion in TBS group (**A**) and reduced astrocyte staining, particularly at the white matter border with the lesion in F-DS-NT3 (1000 ng/mL) (**D**). **E**. GFAP density at the lesion border with the white and gray matter of the intact cord. * denotes $p<0.05$ vs. TBS control group. Error bars represent standard error of the mean.

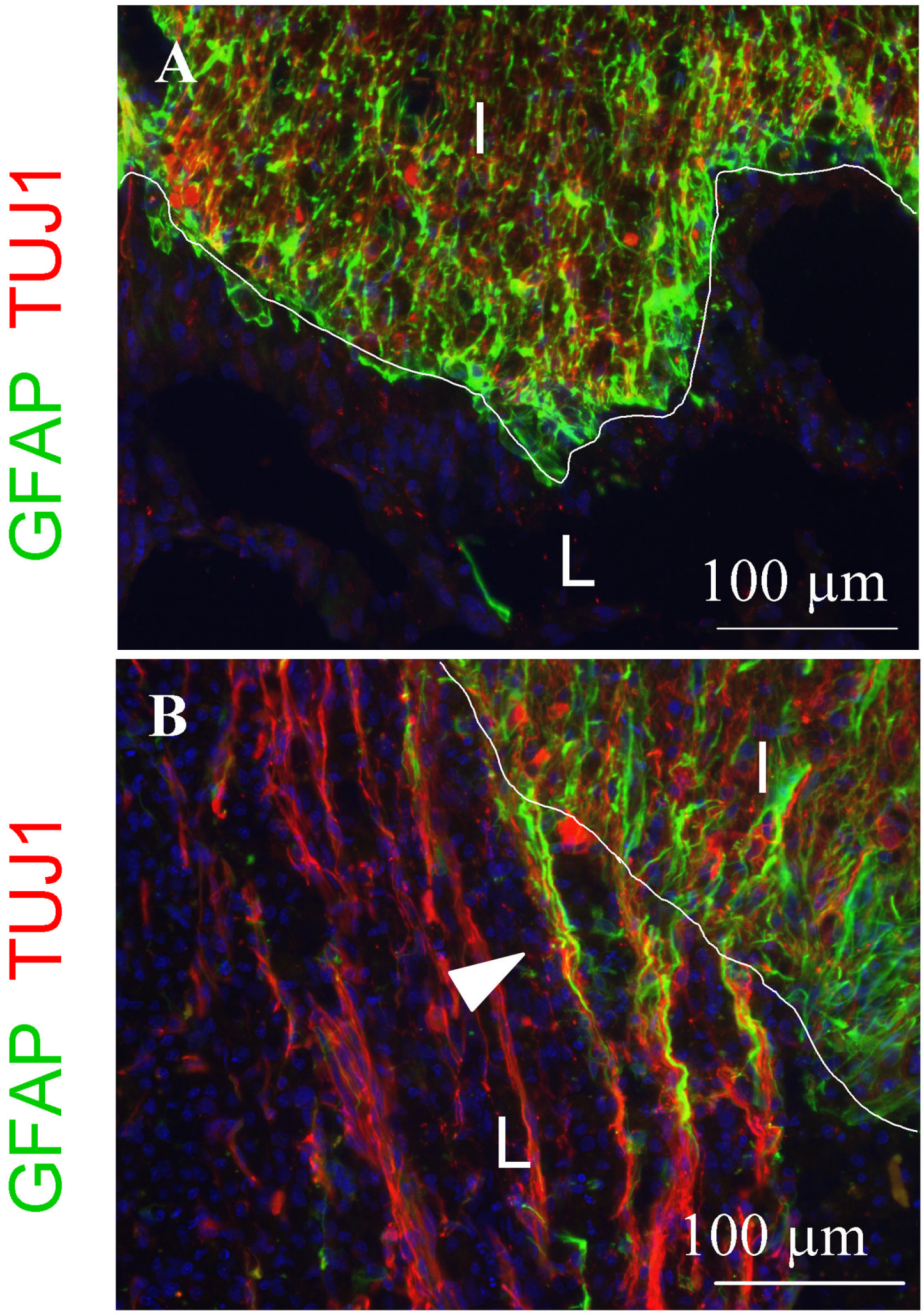

Figure 4.
Infiltration of (**A**) TBS and (**B**) F-DS-NT3(1000 ng/mL) treated cords by neurons and astrocytes. In all panels, blue is Hoechst nuclear stain. Horizontal sections. **A, B.** Neuronal fiber (Tuj1, red) and astrocyte (GFAP, green) double staining at rostral border of gray matter with the lesion. I, intact cord; L, lesion; border indicated by white line. Arrowhead indicates neuronal fiber sprouting into lesion along elongated astrocytes processes.

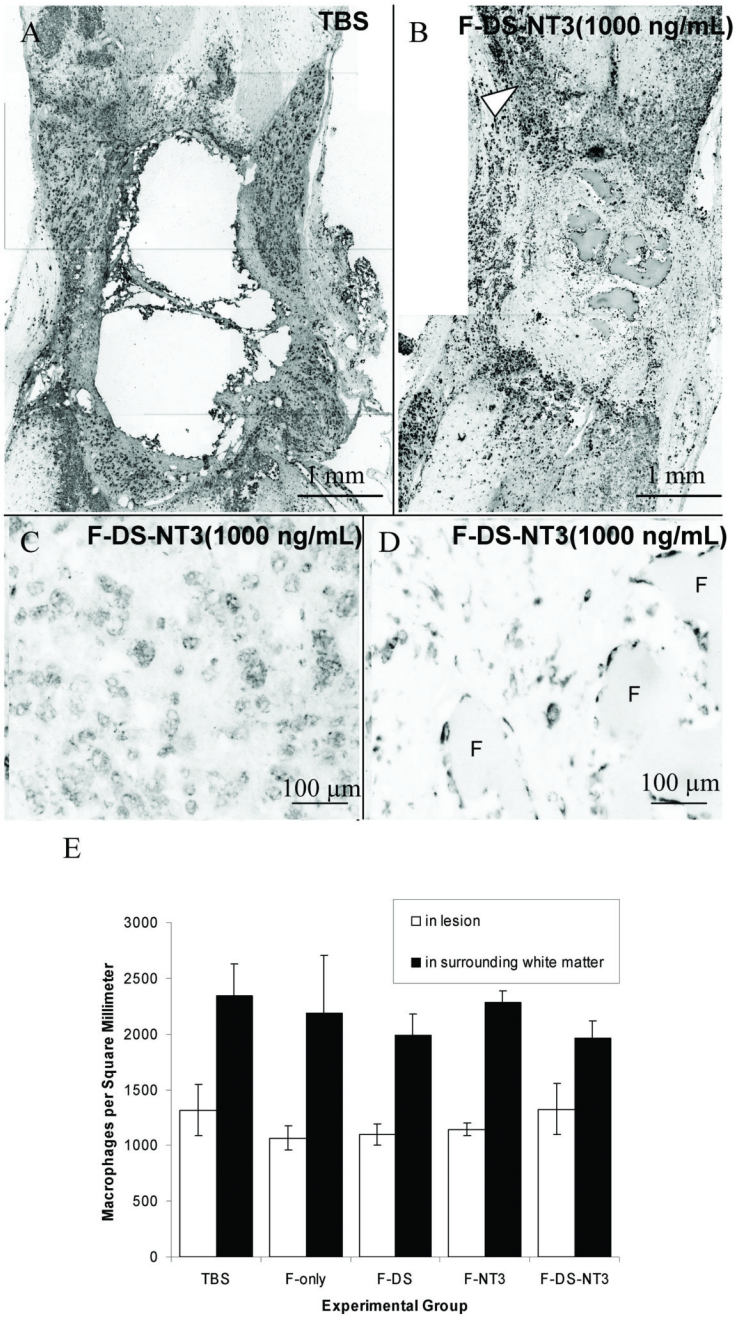

Figure 5.

Effect of fibrin scaffolds on macrophage/microglia density. **A-D**. Macrophage/microglia (ED-1) staining of TBS (**A**) and F-DS-NT-3(1000 ng/mL) (**B-D**) treated cords. Horizontal sections, with the rostral cord oriented toward to top. Arrowhead indicates dense macrophages at white matter border with the lesion site. **C**. White matter border with the lesion site. **D**. Inside the lesion near remaining fibrin scaffold (F). **E**. Density of macrophage/microglia inside lesion and in surrounding white matter. No differences in macrophage/microglia density either in the surrounding white matter or inside the lesion were observed between groups. Error bars indicate standard error of the mean.

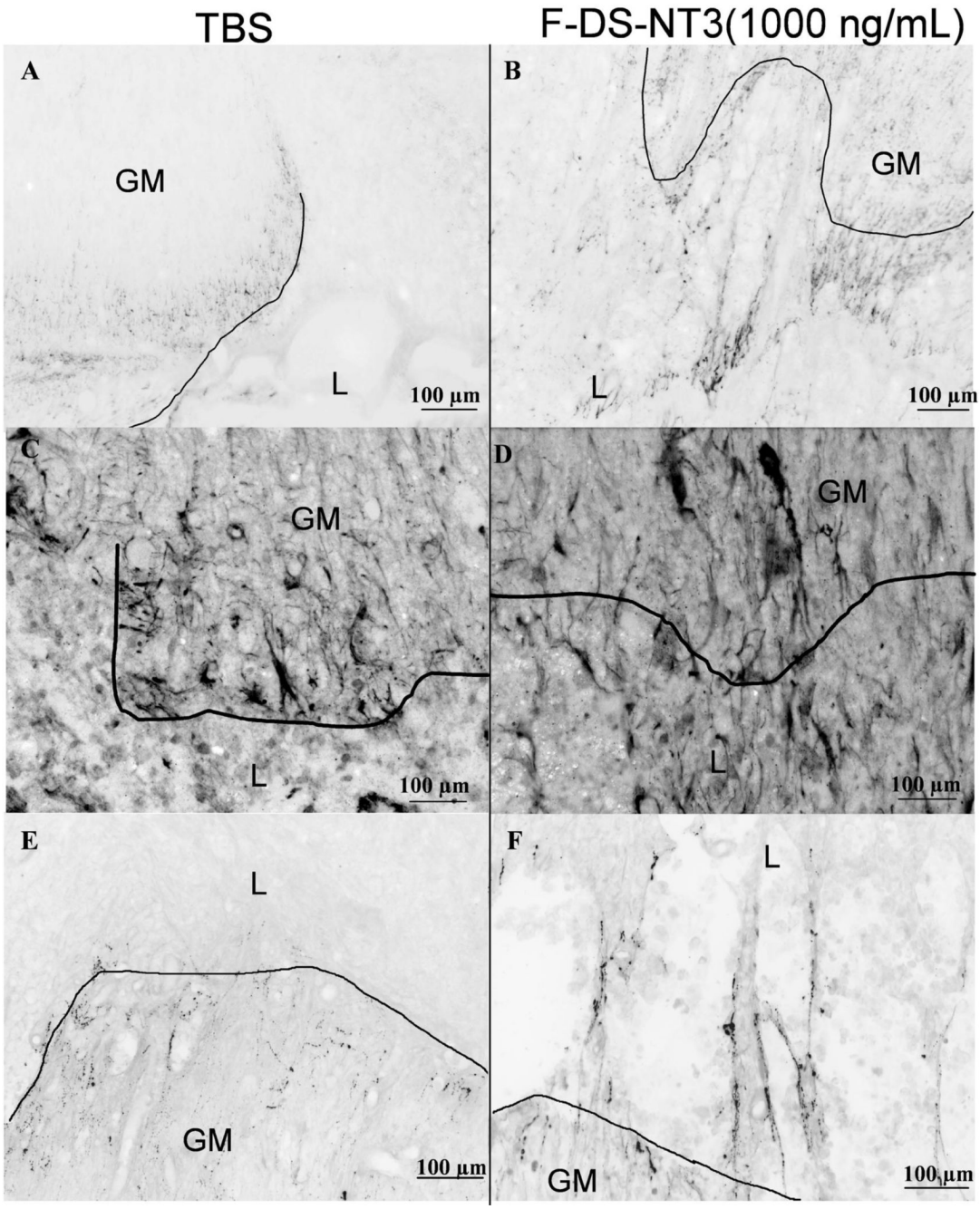

Figure 6.

Effect of fibrin scaffolds on neuronal subpopulations. Horizontal sections, with the rostral cord oriented toward to bottom. **A,B**. Sensory neuron staining (calcitonin gene related peptide, CGRP) of TBS (**A**) and F-DS-NT-3(1000 ng/mL) (**B**) treated cords. Caudal cord shown. **C,D**. Cholinergic (ChAT) staining of lesions of TBS (**C**) and F-DS-NT-3(1000 ng/mL) (**D**) treated cords. Caudal cord shown. **E, F**. Serotonergic (5-HT) staining of lesions of TBS (**E**) and F-DS-NT-3(1000 ng/mL) (**F**) treated cords. Rostral cord shown. GM, gray matter; L, lesion; border indicated by line.

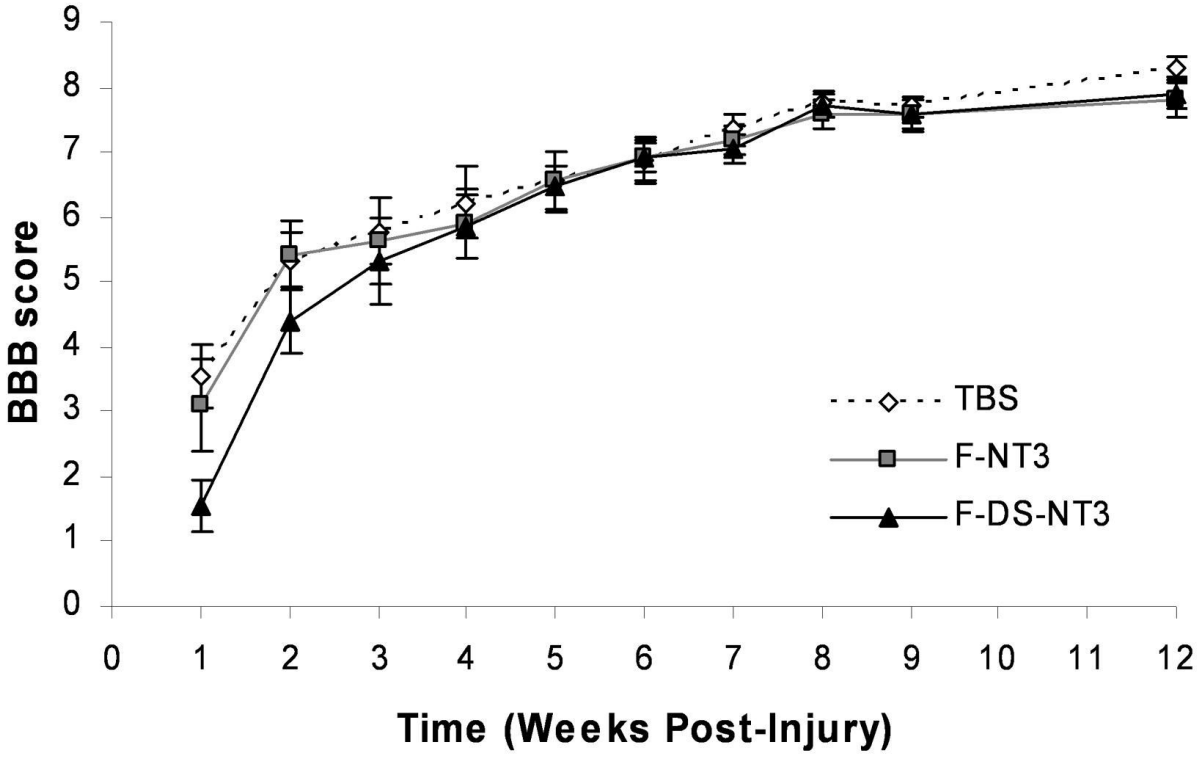

Figure 7.
Functional assessment of SCI with BBB testing in 12-week study. One week after injury, slight or extensive movement of two or three joints was regained, as indicated by a BBB score of 2-3 (a score of 21 indicates unimpaired hindlimb movement). No statistical differences were seen between groups. Error bars represent standard error of the mean.